2020 IEEE REGION 10 CONFERENCE (TENCON)
Osaka, Japan, November 16-19, 2020

Automatic Anchor Calibration for UWB-based Indoor Positioning Systems

Yukiya Yasukawa
Division of Mechanodesign
Kyoto Institute of Technology
Kyoto 606-8585
Email: m0623127@edu.kit.ac.jp

Yoshiyuki Higashi
Faculty of Mechanical Engineering
Kyoto Institute of Technology
Kyoto 606-8585
Email: higashi@kit.ac.jp

Arata Masuda
Center for Manufacturing Technology
Kyoto Institute of Technology
Kyoto 606-8585
Email: masuda@kit.ac.jp

Nanako Miura
Faculty of Mechanical Engineering
Kyoto Institute of Technology
Kyoto 606-8585
Email: miura-n@kit.ac.jp

***Abstract*—In order to navigate Unmanned Aerial Vehicles (UAVs) in GNSS-denied environments localized indoor positioning systems is essential. One of the most common methods for such positioning systems uses high-bandwidth radio frequency called Ultra-wideband (UWB). The UWB radio has several characteristics suited for indoor communication such as low susceptibility to multipath and high immunity against wireless network interference. Although UWB-based positioning is widely used, most of the existing solutions require accurate coordinates of UWB nodes to be known in advance. This put limitation on deployment of positioning systems. In this study, we designed a method to automatically calibrate UWB nodes positions in order to make deployment of indoor positioning systems easier. The proposed method for auto-calibration are tested in real indoor environments to validate effectiveness of the strategy. The effect of node arrangement on accuracy of position estimation was examined as well. As the result, we could improve performance of auto-calibration by changing geometry of UWB nodes.**

***Index Terms*—Ultra-wideband Radio, Indoor positioning systems, Multilateration**

I. Introduction

In recent years Unmanned Aerial Vehicles (UAVs) are promising to play more and more important roles in our society. One of many fields that can be benefited from application of UAVs is inspection of buildings and concrete structures such as bridges. The inspection of structures often involves work at high place which may require special skill for labors. Therefore, developing the new inspection method utilizing UAVs is beneficial.

However, one significant obstacle to using UAVs for the structure inspection is limited performance of UAVs in environment where Global Navigation Satellite Systems (GNSS) are unavailable. Currently, navigation of UAVs is heavily dependent on GNSS [1]. On the other hand, the inspection of structures are expected to be conducted in environments where GNSS signals from satellites can be fully or partially obstructed by surrounding objects, such as indoor and urban environments. In these circumstances, the performance of GNSS suffers from blocked line-of-sights to the satellites and measurement errors caused by reflected signals called multipath propagation. Therefore, more localized positioning systems with high resistance to multipath are instrumental to operate UAVs in indoor and urban environments.

A promising RF technology for such positioning systems is Ultra-wideband (UWB) ranging technology. The UWB radio has several characteristics that suited for indoor communications such as low susceptibility to multipath and high immunity against wireless network interference [2]. To achieve the 3D positioning, a UWB module (tag) is installed on the UAVs to send ranging requests to some fixed UWB nodes at known positions (anchors). Then, position of tag are calculated from anchor positions and distance measurements to the tag.

One of the limitations of UWB-based positioning is that this method require positions of anchors to be known in advance. This can put restrain on applicability of UWB-based positioning in many practical scenarios. Especially in case of inspection of large structures users may need to conduct survey for large amount of anchors in order to install positioning systems. This limitation is significant disadvantage of UWB-based positioning systems when compared with GNSS.

The objective of this study is to design and develop a method to automatically calibrate anchor coordinates without manual inputs from users. To achieve this, we utilized inter-anchor communications of UWB nodes.

II. UWB Ranging

A. UWB radio communications

Ultra-wideband (UWB) is Radio Frequency (RF) signals whose bandwidth is greater than 20 percent of center frequency, or is greater than 500 MHz [3]. This large bandwidth is related to the main characteristics of UWB. UWB communication works by emitting signals as very short pulse with precise timing. This process result in low transmission power which avoid interference to other common radio technologies such as WiFi or BLE. Particularly in distance measurement, the very short pulse modulation gives UWB high immunity to multipath. The multipath is propagation errors caused by radio signals reaching the receiving antenna by two or more paths [4]. Given that the inter pulse period is large enough to differentiate between multiple signals, reflected signals are detected after a main path signal.

978-1-7281-8455-5/20/$31.00 ©2020 IEEE

In this study DWM1000 UWB transceivers are used for UWB communication as commercial-off-the-shelf solution. This and other Decawave devices are the some of the most commonly used modules for UWB ranging [5]. DWM1000 is specialized in measuring distance with a algorithm called Two-way Ranging (TWR). We applied calibration method shown in [6] to obtain higher ranging accuracy.

B. Two-way Ranging method

In this section, we explain how distance can be measured using UWB communication. The two main methods for UWB ranging are time of flight (ToF) and time difference of arrival (TDoA) [7]. The ToF is method that measure time it takes for radio signal to travel between an emitter and a receiver and multiply measured time by speed of light to calculate distance. In TDoA, emitter send out data packets to all nearby receivers and position of an emitter can be calculated by the difference of reception time between each receivers. [8]. In this method all receivers must be time synchronized.

In this study we use the ToF to measure distance and we specifically used algorithm called Two-way Ranging (TWR). This is a well-known technique to deal with clock drift in ToF measurements between unsynchronised devices. Fig. 1 shows principle of the Two-way Ranging algorithm [9]. In order to get a precise distance, three messages (Poll, Response and Final) are exchanged between the ranging initiator (commonly called tag) and the responder (anchor). It is calculated based on the tag timestamps (T_{P1}, T_{R2}, T_{F1}) and the anchor timestamps (T_{P2}, T_{R1}, T_{F2}) as shown in fig. 1.

With these timestamps, the time taken by radio wave communication, ToF is:

$$\begin{aligned} ToF = \frac{1}{4}&((T_{R2} - T_{P1}) - (T_{F1} - T_{R2}) \\ &+(T_{F2} - T_{R1}) - (T_{R1} - T_{P2})) \end{aligned} \tag{1}$$

The distance between the quad-rotor and the anchor d is obtained by multiplying ToF by the speed of light c.

$$d = \text{ToF} \times c \tag{2}$$

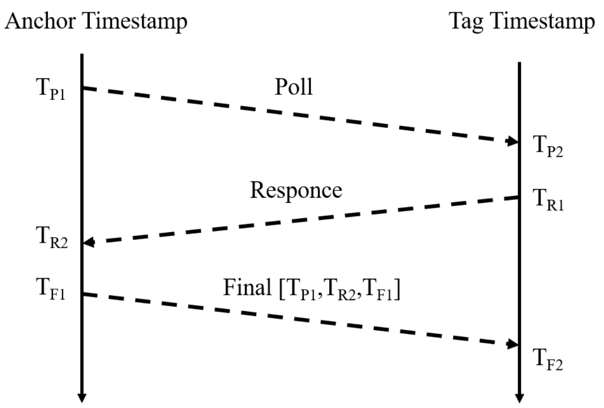

Fig. 1: Principle of Two-way Ranging method.

III. UWB-Based Positioning System

A. Multilateration

After the distance between a tag and anchors are obtained by the UWB ranging, the algorithm called multilateration is applied to calculate position of tag. The multilateration involves the position estimation of an object on its distance from several reference points whose coordinates are known. In very simple scheme, multilateration consist in finding where a group of spheres interact while using known locations of reference points as center coordinates of spheres and measured distances as radius.

When there are specifically three reference points, the algorithm is called trilateration. In this study, we used the Caley-Menger determinant method [10] to solve the trilateration problem. This method is closed-form solution derived entirely from geometrical calculations in Euclidean space. The method has advantage of low computation effort and robustness for errors in input data [11].

The Caley-Menger determinant of two sequence of n points, $[\mathbf{p_1}, \cdots, \mathbf{p_n}]$ and $[\mathbf{q_1}, \cdots, \mathbf{q_n}]$, is defined as:

$$D(\mathbf{p_1}, \cdots, \mathbf{p_n}; \mathbf{q_1}, \cdots, \mathbf{q_n}) =$$
$$2\left(\frac{-1}{2}\right)^n \begin{vmatrix} 0 & 1 & 1 & \cdots & 1 \\ 1 & D(\mathbf{p_1}, \mathbf{q_1}) & D(\mathbf{p_1}, \mathbf{q_2}) & \cdots & D(\mathbf{p_1}, \mathbf{q_n}) \\ 1 & D(\mathbf{p_2}, \mathbf{q_1}) & D(\mathbf{p_2}, \mathbf{q_2}) & \cdots & D(\mathbf{p_2}, \mathbf{q_n}) \\ \vdots & \vdots & \vdots & \ddots & \vdots \\ 1 & D(\mathbf{p_n}, \mathbf{q_1}) & D(\mathbf{p_n}, \mathbf{q_2}) & \cdots & D(\mathbf{p_n}, \mathbf{q_n}) \end{vmatrix} \tag{3}$$

where $D(\mathbf{p_i}, \mathbf{q_i})$ denotes the squared distance between the points $\mathbf{p_i}$ and $\mathbf{q_i}$.

Using Caley-Menger determinant, for reference points $\mathbf{p_1}, \mathbf{p_2}$ and $\mathbf{p_3}$, unknown point $\mathbf{p_4}$ is given by :

$$\mathbf{p_4} = \mathbf{p_1} + k_1\mathbf{v_1} + k_2\mathbf{v_2} \pm k_3(\mathbf{v_1} \times \mathbf{v_2}) \tag{4}$$
$$\tag{5}$$

$\mathbf{v_1}$ and $\mathbf{v_2}$ are vectors defined as:

$$\mathbf{v_1} = p_2 - p_1 \tag{6}$$
$$\mathbf{v_2} = p_3 - p_1 \tag{7}$$

The constants k_1, k_2 and k_3 are calculated by means of Caley-Menger determinants $D(\cdot)$ as:

$$k_1 = -\frac{D(\mathbf{p_1}, \mathbf{p_2}, \mathbf{p_3}; \mathbf{p_1}, \mathbf{p_3}, \mathbf{p_4})}{D(\mathbf{p_1}, \mathbf{p_2}, \mathbf{p_3}; \mathbf{p_1}, \mathbf{p_2}, \mathbf{p_3})} \tag{8}$$
$$k_2 = \frac{D(\mathbf{p_1}, \mathbf{p_2}, \mathbf{p_3}; \mathbf{p_1}, \mathbf{p_2}, \mathbf{p_4})}{D(\mathbf{p_1}, \mathbf{p_2}, \mathbf{p_3}; \mathbf{p_1}, \mathbf{p_2}, \mathbf{p_3})} \tag{9}$$
$$k_3 = \frac{+\sqrt{D(\mathbf{p_1}, \mathbf{p_2}, \mathbf{p_3}, \mathbf{p_4})}}{D(\mathbf{p_1}, \mathbf{p_2}, \mathbf{p_3}; \mathbf{p_1}, \mathbf{p_2}, \mathbf{p_3})} \tag{10}$$

k_1, k_2 and k_3 set a scaling factor in the directions required to have the position p_4 located. The trilateration variables are shown in fig. 2.

B. Dilution of precision

The performance of the multilateration is heavily affected by the range errors and geometrical arrangement of the anchors and a tag. This effect caused by geometry is called Dilution of Precision (DOP) [12]. DOP is important factor to consider when planing deployment of anchors for positioning systems as DOP gives the effect of anchor geometry on accuracy of position estimation .

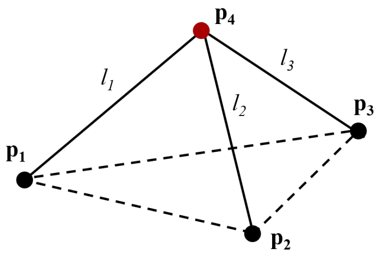

Fig. 2: Trilateration variables, positions $\mathbf{p_i}$, and distances l_i. With Caley-Menger determinant denotation, $l_i^2 = D(\mathbf{p_i}, \mathbf{p_4})$

DOP amplify range error and propagate error when position is computed. In general, a lower DOP value indicate higher accuracy of position estimation. DOP is dimensionless value and only affected by geometry of anchors. The distance between anchors does not affect DOP.

In case of trilateration, DOP can be calculated by following equation. [13]. The three anchors $\mathbf{p_1} = (x_1, y_1, z_1)$, $\mathbf{p_2} = (x_2, y_2, z_2)$, $\mathbf{p_3} = (x_3, y_3, z_3)$ and the range measurement l_1, l_2, l_3 to the unknown point p_4 are given. When coodinate of tag $\mathbf{p_4}$ is defined as $\mathbf{p_4} = (x, y, z)$ DOP is given as:

$$\mathbf{D} = \begin{bmatrix} (x-x_1)/l_1 & (y-y_1)/l_1 & (z-z_1)/l_1 \\ (x-x_2)/l_2 & (y-y_2)/l_2 & (z-z_2)/l_2 \\ (x-x_3)/l_3 & (y-y_3)/l_3 & (z-z_3)/l_3 \end{bmatrix} \quad (11)$$

$$\mathbf{Q} = (\mathbf{D^T} \cdot \mathbf{D})^{-1} = \begin{bmatrix} XDOP^2 & & \\ & YDOP^2 & \\ & & ZDOP^2 \end{bmatrix} \quad (12)$$

The off-diagonal terms are not shown for clarity. The each one of diagonal terms gives the square of DOP value for X, Y, Z direction.

Fig. 3 and fig. 4 are examples of calculated DOP as a color contour maps when anchors are arranged as a equilateral triangle. The lower the DOP value, the better the accuracy of positioning. The coordinates of the anchors are given as $\mathbf{p_1} = (-1000\sqrt{3}, -1000, 0)$, $\mathbf{p_2} = (0, 2000, 0)$, $\mathbf{p_3} = (1000\sqrt{3}, -1000, 0)$. The calculation area for fig. 3 is an XY plane at height of 1400. It can be seen that positioning accuracy will be higher at center of a triangle.

The height of tag has significant effect on DOP as well. The calculation area for fig. 4 is an XZ plane at Y=0. The DOP for vertical direction (=ZDOP) is specially affected by tag height. The closer a tag is to anchor plane, the higher the DOP become.

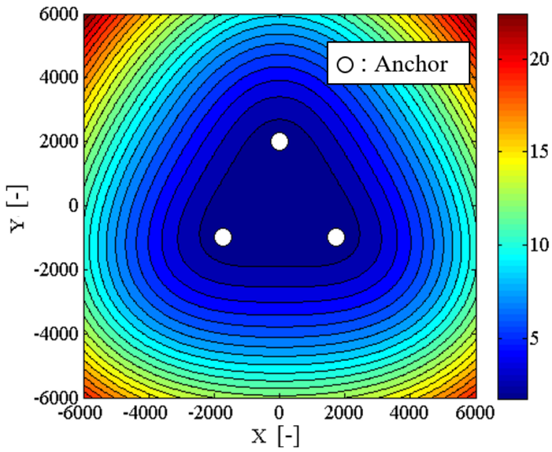

Fig. 3: Color contour map of DOP when anchors are arranged as equilateral triangle

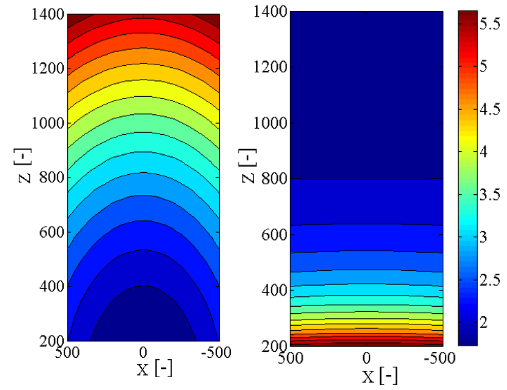

(1)Horizontal DOP (2)Vertical DOP

Fig. 4: Effect of tag height on DOP

C. Auto-calibration of anchors

The main objective of this study is to make deployment of UWB-based positioning systems easier by automatic calibration of anchor coordinates. This section explains the auto-calibration process that utilizes UWB inter-anchor communication.

First, coordinates of at least three anchors must be defined, in this study we determine coordinates of initial anchors by UWB ranging or GNSS depend on surrounding environment.

The UWB ranging can be used in indoor environment where satellite signals are completely blocked. In these environments, coordinates of anchors can be determined by algorithm shown in [14]. In this method, all three UWB anchors are assumed to be placed at the same height. This requirement can limit applicability of this method in certain environment where ground is not paved properly.

The usage of GNSS is preferable when anchors are deployed in urban or semi-indoor environment. For example, llet us consider inspection of bridge using UAVs. When the UAVs are flying under the bridge, GNSS is impractical for navigation since satellite signals are largely obstructed by the structure. However, even in an environment like this we can still utilize GNSS by placing anchor nodes in open area where satellite signals are available. Then, the location information obtained from GNSS can be used as reference points for position estimation of other UWB anchors. An advantage of this method over aforementioned UWB ranging method is how there are no constraints on placement of anchors as long as GNSS signals are available.

After position of three anchors are determined, coverage of positioning systems can be expanded by placing another anchors. The newly placed anchors can communicate with initial three anchor to measure distance. The positions of new anchors can be estimated by applying multilateration while using initial three anchors as reference points. When UWB-based positioning systems are deployed across large area, coverage of positioning systems can be further expanded by repeating multilateration while using the anchors that calibrated in previous step as reference points.

IV. Experiment and Performance Evaluation

A. Effect of initial anchors determination method

As mentioned earlier, this auto-calibration process can utilize both GNSS and UWB ranging for determination of initial three anchor positions depend on condition of surrounding environment. To validate two method for initial anchor determination, experiment have been conducted.

We deployed UWB nodes in outdoor environment and arrange them as shown in fig. 5. First, coordinates of anchor nodes A_1, A_2, A_3 have been surveyed either by GNSS or by UWB ranging. Next, tag nodes T_1-T_4 measure the distance from each anchor nodes. Finally, coordinate of tag nodes was calculated using multilateration.

The result of initial anchor determination by GNSS is shown in table I and by UWB ranging is shown in table II. In both method, maximum position errors did not exceed 70 mm.

Next, the estimated position of tag in case of GNSS was used for initial determination are shown in table III and case for UWB ranging are shown in table IV. The estimation results of two method show similar degree of errors. Thus, both GNSS and UWB ranging can be valid method for initial anchors determination.

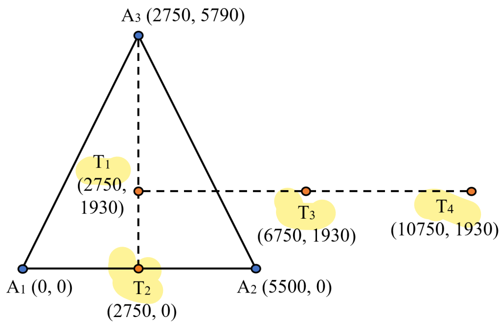

Fig. 5: Arrangement of UWB nodes in initial anchor determination experiment.

TABLE I: Result of anchor position determination by GNSS

Anchor	Position Errors[mm]		
	X	*Y*	*Z*
A_1	0	0	0
A_2	31	0	48
A_3	41	10	-69

TABLE II: Result of anchor position determination by UWB ranging

Anchor	Position Errors[mm]		
	X	*Y*	*Z*
A_1	0	0	0
A_2	-4	0	0
A_3	44	13	0

TABLE III: Estimation errors of Tags (Anchor position determined by GNSS)

Tag	Position Errors[mm]		
	X	*Y*	*Z*
T_1	73	60	173
T_2	-1	60	204
T_3	-8	-37	212
T_4	-182	47	1611

TABLE IV: Estimation errors of Tags (Anchor position determined by UWB ranging)

Tag	Position Errors[mm]		
	X	*Y*	*Z*
T_1	64	58	179
T_2	-16	58	180
T_3	2	-44	239
T_4	-136	4	1337

B. Performance evaluation of anchor auto-calibration

The aim of our work is to enable inspection of large structures using UWB-based positioning systems. To realize this, the network of UWB nodes must be expanded beyond coverage of initial three anchors using proposed auto-calibration method. However, in the process of repeated multilateration, measurement errors and calculation errors are expected to accumulate and affect accuracy of position estimation.

To investigate degradation of accuracy through expansion of positioning systems, experiment was conducted in an indoor environment on Kyoto Institute of Technology's campus. As for hardware, we used Decawave's DWM1000 for UWB communication and Espressif Systems's ESP32 micro-controller for running ranging program. Each UWB node can work as both anchor and tag by switching mode via user input. We placed up to three anchors and a tag in the room.

In this experiment, we placed UWB nodes in two-dimensional arrangement at following coordinates.

- P_1 = (0, 0, 0)
- P_2 = (1000, $1000\sqrt{3}$, 0)
- P_3 = (2000, 0, 0)
- P_4 = (3000, $1000\sqrt{3}$, 0)
- P_5 = (4000, 0, 0)
- P_6 = (5000, $1000\sqrt{3}$, 0)
- P_7 = (6000, 0, 0)
- P_8 = (7000, $1000\sqrt{3}$, 0)

- C_1 = (1000, $1000\sqrt{3}/3$, 0)
- C_2 = (2000, $2000\sqrt{3}/3$, 0)
- C_3 = (3000, $1000\sqrt{3}/3$, 0)
- C_4 = (4000, $2000\sqrt{3}/3$, 0)
- C_5 = (5000, $1000\sqrt{3}/3$, 0)
- C_6 = (6000, $2000\sqrt{3}/3$, 0)

Please note that all coordinates are in millimeter. P_1-P_8 are anchor nodes and C_1-C_5 are tag nodes. The anchors and the tags are arranged in the way that horizontal DOP will be minimum at each tag.

First, all anchor positions were calculated by proposed auto-calibration process. Three anchors P_1, P_2 and P_3 work as initial anchors and their accurate positions are known in advance. The coordinate of anchor P_4 can be calculated by multilateration based on distance between unknown point P_4 and known points P_1, P_2 and P_3. After position of P_4 is estimated, position of another anchor P_5 can be calculated by P_4 as new reference point. By repeating this procedure, coordinate of all anchors can be estimated.

After coordinates of all anchor nodes are defined, positions of tag nodes are estimated to validate the performance of expanded positioning systems. The tags are placed inside each expanded coverage areas and communicate with nearest three anchors to measure distances.

Fig. 7 shows estimated position of both auto-calibrated anchors and tags. The results of anchor auto-calibration are shown in table V. The estimation results of tags are shown in table VI.

As expected, the propagated errors were accumulated during expansion of anchor coverage. Due to low Horizontal DOP of this particular arrangement, errors for X and Y axis are relatively small. However, since all anchors and tags are placed at same height, Vertical DOP are notably high and as a result error for Z axis increased. This Z error was propagated every times each anchors are used as reference point for multilateration and because of this, position errors gradually increased in each step of expansion. As a consequence of anchor calibration errors, accuracy of position estimation for tags are significantly decreased as well.

C. Effect of anchor arrangement on the error accumulation

The previous experiment showed significant increase of errors after expansions of anchor coverage. One of the probable causes for such large errors are DOP. Particularly Vertical DOP is very high with arrangement of anchors used in the previous experiment. Thus, performance of anchor auto-calibration can be improved by better arrangement of anchors. In this experiment, we deployed the anchors in three-dimensional arrangement where DOP is expected to be lower than two-dimensional arrangement in previous experiment. Fig. 6 show experiment setup for three dimensional anchor arrangement. The anchors were placed at following coordinates. The tags coordinates are same as previous experiment.

TABLE V: Errors of estimated anchor positions in two-dimensional arrangement

Anchor	Position Errors[mm]			
	X	*Y*	*Z*	*XYZ*
P_4	119.7	61.1	786.8	798.2
P_5	-214.4	-95.0	947.8	976.4
P_6	-672.6	-483.3	2368.7	2509.3
P_7	-1419	-789.2	2896.9	3320.9
P_8	-2525.6	-970.0	4279.3	5062.8

TABLE VI: Errors of estimated tag positions in two-dimensional arrangement

Tag	Position Errors[mm]			
	X	*Y*	*Z*	*XYZ*
C_1	-55.2	-6.6	115.4	128.1
C_2	-20.2	-22.4	678.8	679.5
C_3	-283.7	34.2	951.8	993.8
C_4	-355.2	-188.6	1432.1	1487.5
C_5	-1095.2	-490.8	2264.8	2563.1
C_6	-1778.6	-801.0	3226.3	3770.1

TABLE VII: Errors of estimated anchor positions in three-dimensional arrangement

Anchor	Position Errors[mm]			
	X	*Y*	*Z*	*XYZ*
P_{3l}	-95.6	-370.6	-6.2	382.8
P_{3h}	-24.8	-134.9	122.2	183.7
P_4	-6.9	14.6	-50.6	53.1
P_{5l}	-128.4	-371.2	-26.5	393.7
P_{5h}	-52.6	-327.4	-12.8	331.9
P_6	15.4	-68.5	-68.8	98.3
P_{7l}	-183.0	-409.6	-188.2	486.5
P_{7h}	-40.7	-418.4	-83.4	428.5
P_8	-40.7	-77.0	-171.4	192.2

TABLE VIII: Errors of estimated tag positions in three-dimensional arrangement

Tag	Position Errors[mm]			
	X	*Y*	*Z*	*XYZ*
C_1	206.7	-167.6	14.1	266.5
C_2	-95.4	-119.6	-41.2	158.4
C_3	-122.5	-141.4	41.9	191.7
C_4	-94.5	-161.1	26.7	188.7
C_5	-126.3	-228.3	-3.6	260.9
C_6	-132.1	-235.1	-51.2	274.5

- P_{1l} = (0, 0, -1000)
- P_{1h} = (0, 0, 1000)
- P_2 = (1000, $1000\sqrt{3}$, 0)
- P_{3l} = (2000, 0, -1000)
- P_{3h} = (2000, 0, 1000)
- P_4 = (3000, $1000\sqrt{3}$, 0)
- P_{5l} = (4000, 0, -1000)
- P_{5h} = (4000, 0, 1000)
- P_6 = (5000, $1000\sqrt{3}$, 0)
- P_{7l} = (6000, 0, -1000)
- P_{7h} = (6000, 0, 1000)
- P_8 = (7000, $1000\sqrt{3}$, 0)

Fig. 8 shows estimated position of both anchors and tags. The results of anchor auto-calibration are shown in table VII. The estimation results of tags are shown in table VIII. The estimated positions of both anchors and tags show significant improvement in accuracy compared to previous experiment with two-dimensional anchor arrangement.

V. Conclusion

In order to make navigation of UAVs in GNSS denied environment more practical, we proposed a method to

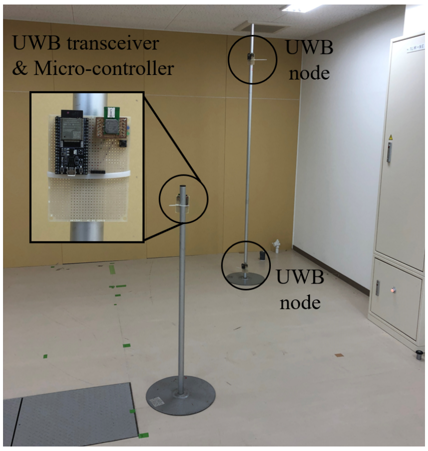

Fig. 6: Experiment setup for three dimensional anchor arrangement

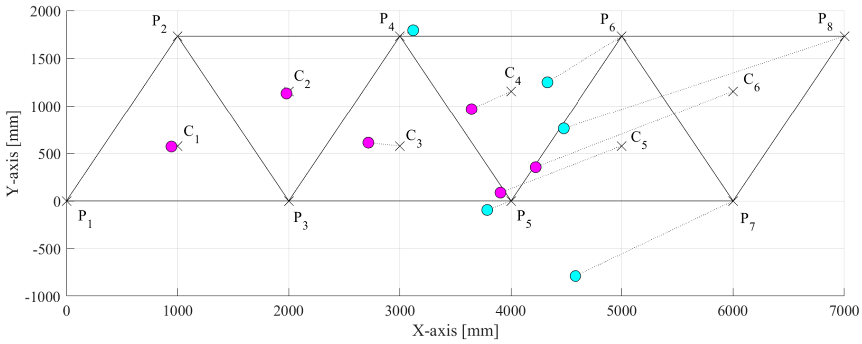

Fig. 7: Estimated position of anchors (blue) and. tags (red) in two-dimensional arrangement

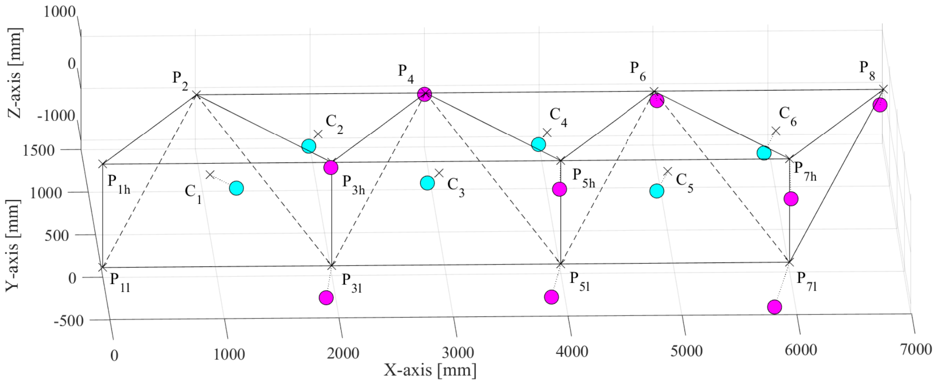

Fig. 8: Estimated position of anchors (blue) and. tags (red) in three-dimensional arrangement

make deployment of anchors for UWB-based positioning system easier by automatic survey of anchor coordinates. This method utilizes inter-anchor communication to measure distance between the anchors and applies multilateration to determine their location. Automatic calibration of anchors eliminates necessity to survey anchor coordinates in advance.

Multilateration requires coordinates of at least three anchors to be known beforehand. To determine initial three anchors position, two approaches which utilizes either GNSS or measurement of inter-anchor distance are proposed. Both methods were found to be sufficiently accurate for following multilateration step. After iterations of inter-anchor positioning, the position errors are expected to accumulate over time. We conducted experiments to validate degradation of accuracy after expansion of positioning system. As the result of three-dimensional arrangement of anchors, accumulated errors could be greatly reduced.

Acknowledgment

This work was supported by JSPS KAKENHI Grant Number JP 20K04379.

References

[1] A. R. Kuroswiski, N. M. F. de Oliveira and É. H. Shiguemori, "Autonomous long-range navigation in GNSS-denied environment with low-cost UAV platform," 2018 Annual IEEE International Systems Conference (SysCon), Vancouver, BC, pp. 1-6, 2018, doi: 10.1109/SYSCON.2018.8369592.

[2] A. Alarifi, A. Al-Salman, M. Alsaleh, A. Alnafessah, S. Al-Hadhrami, M. A. Al-Ammar, and H. S. Al-Khalifa, "Ultra Wideband Indoor Positioning Technologies: Analysis and Recent Advances." Sensors (Basel, Switzerland), 16(5), 707. 2016, doi: 10.3390/s16050707.

[3] G. M. Mendoza-Silva, J. Torres-Sospedra, J. Huerta, 2019. "A Meta-Review of Indoor Positioning Systems." Sensors 19, no. 20: 4507.

[4] S. Geng, S. Ranvier, X. Zhao, J. Kivinen and P. Vainikainen, "Multipath propagation characterization of ultra-wide band indoor radio channels," 2005 IEEE International Conference on Ultra-Wideband, Zurich, Switzerland, 2005, pp. 11-15, doi: 10.1109/ICU.2005.1569948.

[5] P. Dawei and Y. Yunhua. "Design of Indoor Position System Based on DWM1000 Modules." IOP Conference Series: Materials Science and Engineering. 585. 012067. 2019, doi: 10.1088/1757-899X/585/1/012067.

[6] K. Guo, Z. Qiu, C. Miao, A.H. Zaini, C. Chen, W. Meng, and L. Xie, "Ultra-Wideband-Based Localization for Quadcopter Navigation. " Unmanned Syst. 4, pp. 23-34, 2016.

[7] A. Ledergerber, M. Hamer and R. D'Andrea, "A robot self-localization system using one-way ultra-wideband communication," 2015 IEEE/RSJ International Conference on Intelligent Robots and Systems (IROS), Hamburg, pp. 3131-3137, 2015, doi: 10.1109/IROS.2015.7353810.

[8] Z. Wei, X. Chen, L. Fang, N. Zhao, S. Guo and X. Li, "Joint positioning technique based on TOF and TDOA," 2018 IEEE International Instrumentation and Measurement Technology Conference (I2MTC), Houston, TX, 2018, pp. 1-6, doi: 10.1109/I2MTC.2018.8409683.

[9] S. Akahori, Y. Higashi and A. Masuda, "Position estimation system with UWB, IMU and a distance sensor for quad-rotors," TENCON 2017 - 2017 IEEE Region 10 Conference, Penang, 2017, pp. 1992-1996, doi: 10.1109/TENCON.2017.8228187.

[10] F. Thomas and L. Ros, "Revisiting trilateration for robot localization," in IEEE Transactions on Robotics, vol. 21, no. 1, pp. 93-101, Feb. 2005, doi: 10.1109/TRO.2004.833793.

[11] K. Befus, "Localization and System Identification of a Quadcopter UAV". Master's Theses. 499. 2014.

[12] D. E. Manolakis, "Efficient solution and performance analysis of 3-D position estimation by trilateration," in IEEE Transactions on Aerospace and Electronic Systems, vol. 32, no. 4, pp. 1239-1248, Oct. 1996, doi: 10.1109/7.543845.

[13] M. Yuen, "Dilution of Precision (DOP) Calculation for Mission Planning Purposes", Naval Postgraduate School ,221, 2009.

[14] K. Cisek, A. Zolich, K. Klausen and T. A. Johansen, "Ultra-wide band Real time Location Systems: Practical implementation and UAV performance evaluation," 2017 Workshop on Research, Education and Development of Unmanned Aerial Systems (RED-UAS), Linkoping, pp. 204-209, 2017, doi: 10.1109/RED-UAS.2017.8101667.